APPLIED AND ENVIRONMENTAL MICROBIOLOGY, Dec. 2007, p. 7898–7905 Vol. 73, No. 24
0099-2240/07/$08.00+0 doi:10.1128/AEM.01296-07

Production of Eight Different Hydride Complexes and Nitrite Release from 2,4,6-Trinitrotoluene by *Yarrowia lipolytica*▽†

Ayrat M. Ziganshin,[1,5] Robin Gerlach,[1,2]* Thomas Borch,[3] Anatoly V. Naumov,[4] and Rimma P. Naumova[5]

Center for Biofilm Engineering,[1] Department of Chemical and Biological Engineering,[2] and Department of Chemistry and Biochemistry,[4] Montana State University, Bozeman, Montana 59717; Department of Soil and Crop Sciences, Colorado State University, Fort Collins, Colorado 80523[3]; and Department of Microbiology, Kazan State University, Kazan 420008, Russia[5]

Received 11 June 2007/Accepted 5 October 2007

2,4,6-Trinitrotoluene (TNT) transformation by the yeast strain *Yarrowia lipolytica* AN-L15 was shown to occur via two different pathways. Direct aromatic ring reduction was the predominant mechanism of TNT transformation, while nitro group reduction was observed to be a minor pathway. Although growth of *Y. lipolytica* AN-L15 was inhibited initially in the presence of TNT, TNT transformation was observed, indicating that the enzymes necessary for TNT reduction were present initially. Aromatic ring reduction resulted in the transient accumulation of eight different TNT-hydride complexes, which were characterized using high-performance liquid chromatography, UV-visible diode array detection, and negative-mode atmospheric pressure chemical ionization mass spectrometry (APCI-MS). APCI-MS analysis revealed three different groups of TNT-hydride complexes with molecular ions at *m/z* 227, 228, and 230, which correspond to TNT-mono- and dihydride complexes and protonated dihydride isomers, respectively. One of the three protonated dihydride complex isomers detected appears to release nitrite in the presence of strain AN-L15. This release of nitrite is of particular interest since it can provide a pathway towards complete degradation and detoxification of TNT.

2,4,6-Trinitrotoluene (TNT) is a major component of many explosives. The large-scale production of TNT during the last century led to extensive pollution of soils, surface water, and groundwater (15, 16). TNT is a U.S. Environmental Protection Agency priority pollutant, and therefore pollution prevention and remediation are obligatory at many production and testing sites (4, 10).

Reductive attack on TNT's nitro groups appears to be the dominant mechanism of TNT conversion by most microorganisms (references 2, 4, 7, 8, 12, 13, and 23 and references therein). The possibility of direct aromatic ring reduction of TNT has received much less attention despite the fact that denitration (release of nitrite) and aromatic ring destruction are more likely (9, 14, 21). Direct aromatic ring reduction (often also termed "hydride ion addition"), generally observed at the C-3 position of the aromatic ring, results in the appearance of a TNT-monohydride complex (3-H^--TNT, a deep red metabolite). Stenuit et al. (18) proposed three isomeric structures for 3-H^--TNT, but clear analytical evidence for all three isomers was not obtained. Further aromatic ring reduction of 3-H^--TNT can result in the formation of a dihydride complex (3,5-2H^--TNT), whose pH-dependent protonation has been proposed to lead to three additional isomers (3,5-2H^--TNT·H^+) (19, 20). Characterization of 3-H^--TNT and 3,5-2H^--TNT using negative-mode electrospray ionization mass spectrometry (MS) and nuclear magnetic resonance spectroscopy was performed by Vorbeck et al. (19, 20), and temporal changes in the nuclear magnetic resonance spectra suggested that three protonated forms of 3,5-2H^--TNT (3,5-2H^--TNT·H^+) occur.

Subsequent research in the same and other laboratories resulted in the isolation of a limited number of other microorganisms, both prokaryotes and eukaryotes, capable of carrying out TNT aromatic ring reduction, including *Rhodococcus opacus* HL PM-1 (20), *Enterobacter cloacae* PB (5), *Pseudomonas fluorescens* I-C (14), *Candida* strains (24), *Irpex lacteus* (11), and *Yarrowia lipolytica* NCIM 3589 (9). TNT aromatic ring reduction accompanied by hydride complex formation can lead to the release of nitrite from 3-H^--TNT, resulting in the production of 2,4-dinitrotoluene (2,4-DNT) (9). In addition, the liberation of nitrite from the protonated dihydride complexes is believed to result in the destruction of the TNT aromatic system, leading to the production of alcohols or ketones (21) or to the formation of amino-dimethyl-tetranitrobiphenyls (ADMTNBs) (14).

In order to understand and subsequently optimize the destruction of TNT, it is important to study the initial conversion of TNT during hydride ion addition. Unfortunately, the remaining difficulties in separating the already described and suggested TNT ring reduction products have kept our understanding of TNT transformation by these organisms at an inadequate level (14, 20, 21). The research presented here utilized an improved high-performance liquid chromatography (HPLC)–diode array detection–MS method for the separation of 3,5-2H^--TNT from its 3,5-2H^-TNT·H^+ isomers and resulted in the detection and characterization of three additional TNT-hydride complexes which have not been described previ-

* Corresponding author. Mailing address: Center for Biofilm Engineering, Department of Chemical and Biological Engineering, Montana State University, Bozeman, MT 59717. Phone: (406) 994-1840. Fax: (406) 994-6098. E-mail: robin_g@coe.montana.edu.

† Supplemental material for this article may be found at http://aem.asm.org/.

▽ Published ahead of print on 12 October 2007.

ously. In turn, this research allowed a better understanding the role of hydride complexes in TNT transformation and the elimination of nitro groups by *Y. lipolytica* AN-L15 and other organisms.

MATERIALS AND METHODS

Chemicals. TNT (purity, 99%) was purchased from ChemService (West Chester, PA); 2-amino-4,6-dinitrotoluene (2-ADNT) and 4-amino-2,6-dinitrotoluene (4-ADNT) (purity, 99%) were obtained from Supelco (Bellefonte, PA); 2-hydroxylamino-4,6-dinitrotoluene (2-HADNT) (purity, 97.1%) and 4-hydroxylamino-2,6-dinitrotoluene (4-HADNT) (purity, 96%, respectively) were received from AccuStandard (New Haven, CT).

Yeast strain and culture conditions. Experiments were carried out with the yeast strain *Y. lipolytica* AN-L15 isolated in previous work (24) from an oil-polluted peat bog in Langepas (Western Siberia, Russia). *Y. lipolytica* AN-L15 was selected due to its ability to attack TNT via aromatic ring reduction accompanied by nitrite release. For TNT conversion experiments *Y. lipolytica* AN-L15 was grown aerobically for 20 h at 30°C on Sabouraud agar medium containing (per liter) 10 g of glucose, 10 g of peptone, 5 g of yeast extract, 0.25 g of NaCl, and 20 g of agar. AN-L15 cells were harvested, washed with 16 mM phosphate buffer (pH 7.0), and transferred into 250-ml Erlenmeyer flasks containing 50 ml of synthetic medium with the following composition: 28 mM glucose, 7.6 mM $(NH_4)_2SO_4$, 2 mM $MgSO_4$, 9.8 mM Na_2HPO_4, and 6.2 mM KH_2PO_4 (pH 7.0). The initial cell concentration was adjusted to an optical density of 0.2, and growth was measured at 600 nm (A_{600}) with a Spectronic GENESYS 5 spectrophotometer (Milton Roy Company, Rochester, NY) using cell-free culture medium as the reference. TNT was added to a final concentration of 440 μM from an ethanolic stock solution (0.8 ml of 95.6% ethanol in 50 ml of medium), and the flasks were incubated at 30°C without shaking. Samples for HPLC, nitrite, and yeast growth analyses were taken every 6 h.

HPLC. TNT and its metabolites were routinely separated using a Hewlett Packard 1090 high-performance liquid chromatograph with a diode array detector, as well as an Agilent series 1100 high-performance liquid chromatograph equipped with an autosampler, a fraction collector, a diode array detector, a temperature-controlled column compartment, a Supelcosil LC-8 guard column, and a Supelcosil octyl (C-8) column (150 by 4.6 mm; particle size, 5 μm). Metabolite detection occurred at 230, 254, 440, and 476 nm. UV-visible absorbance spectra of every peak were obtained at wavelengths from 190 to 700 nm. Separation was performed at 36 and 50°C as described in detail by Borch and Gerlach (1) after filtration of samples through 0.2-μm filters (Spartan 13/0.2 RC; Whatman). Chromatography at 36°C allowed good separation of 2-HADNT, TNT, and 4-HADNT but resulted in coelution of 4-ADNT and 2,4-DNT. Increasing the separation temperature from 36 to 50°C allowed sufficient chromatographic resolution of 4-ADNT and 2,4-DNT but resulted in coelution of 4-HADNT and TNT. Hence, samples were analyzed at both temperatures in this study.

Negative-mode APCI-MS. Negative-mode atmospheric pressure chemical ionization (APCI) mass spectra of TNT and its metabolites were obtained using a series 6300 Agilent SL ion trap mass spectrometer. MS analysis was performed simultaneously with HPLC separation (HPLC-MS) and separately after fraction collection via direct infusion into the mass spectrometer. For compound identification, fractions of each metabolite were collected at the time that their concentrations were the highest (between 18 and 36 h for 3-H^--TNT and 1-H^--TNT and between 48 and 84 h for the other TNT-mono- and dihydride complexes). The MS parameters were as follows: nitrogen dry gas flow rates, 1 and 7 liters/min depending on the mode of sample infusion (direct infusion and HPLC-MS, respectively); dry gas and vaporizer temperature, 350°C; corona current, −30,000 nA; capillary voltage, 1,800 V; and trap optimized for *m/z* 227.

Ion chromatography. Nitrite concentrations were determined using a Dionex ion chromatograph equipped with a conductivity detector, an IonPac AG9-HC guard column, and an IonPac AS9-HC analytical column. The mobile phase consisted of 9 mM Na_2CO_3 at a flow rate of 1 ml/min; $NaNO_2$ was used as the reference compound.

RESULTS

Growth of *Y. lipolytica* AN-L15. Inoculation of TNT-free medium with *Y. lipolytica* AN-L15 resulted in immediate growth, whereas the presence of 440 μM TNT delayed observable growth by approximately 36 h (Fig. 1A). However, even during this lag phase, TNT-hydride complex production was observed (Fig. 1B and C), and after 96 h, the cell densities were comparable in TNT-free (A_{600}, 2.1) and TNT-containing (A_{600}, 1.9) cultures (Fig. 1A). This indicates that TNT or its initial transformation products delayed yeast growth, although the enzymes capable of TNT reduction appeared to be present.

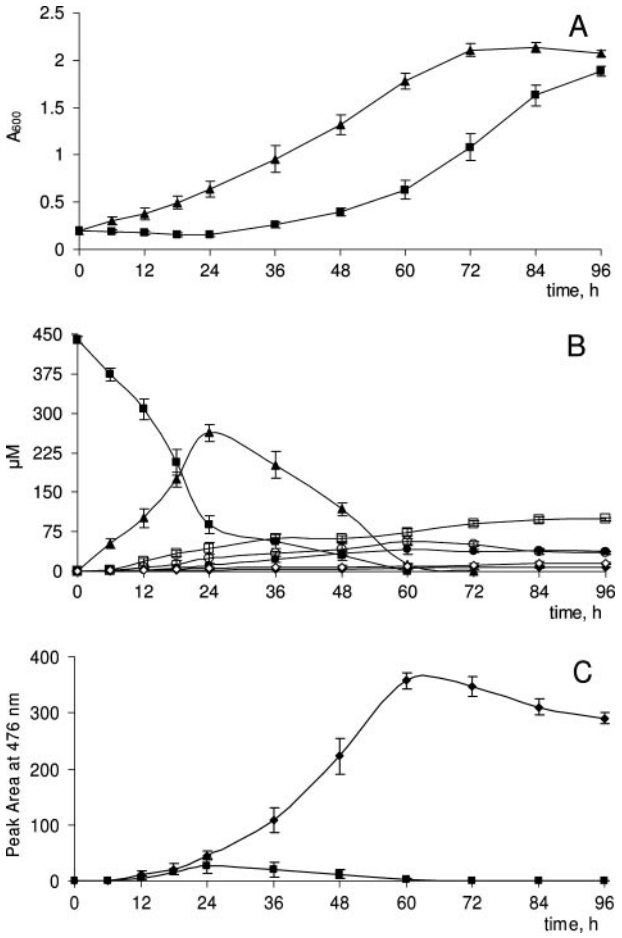

FIG. 1. (A) Growth of *Y. lipolytica* AN-L15. Symbols: ▲, growth in the absence of TNT; ■, growth in the presence of TNT. (B) Accumulation of metabolites during TNT transformation by *Y. lipolytica* AN-L15. Symbols: ■, TNT; ▲, 3-H^--TNT; ●, 2-HADNT; ○, 4-HADNT; ◆, 2-ADNT; ◇, 4-ADNT; □, nitrite. (C) Peak areas. Symbols: ■, 1-H^--TNT; ◆, sum of TNT mono- and dihydride complexes related to 3-H^--TNT (i.e., compounds 1 to 6) expressed as sum of the peak area at 476 nm. The error bars indicate one standard deviation of replicate experiments.

Identification of TNT metabolites. *Y. lipolytica* AN-L15 initiated both nitro group and direct aromatic ring reduction of TNT. Nitro group reduction led to the accumulation of 2-HADNT, 4-HADNT, 2-ADNT, and 4-ADNT, whereas the attack on the aromatic ring resulted in the appearance of eight distinct peaks which were characterized and shown to be mono- and dihydride complexes of TNT.

Figure 2 shows chromatograms of a sample containing all detected metabolites of TNT transformation by *Y. lipolytica* AN-L15 except the amino-dinitrotoluenes (ADNTs) assembled by acquiring signals at two different wavelengths (254 and 476 nm). These two chromatograms show the separation of

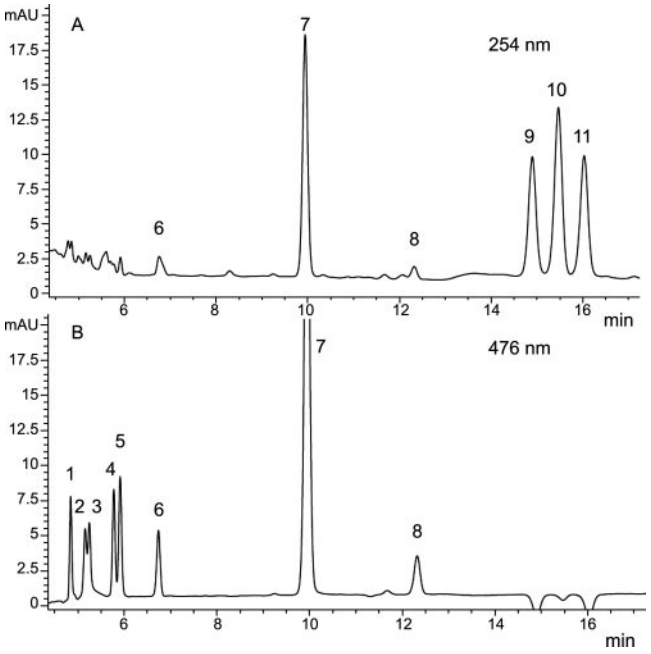

FIG. 2. Separation of metabolites produced during TNT transformation by *Y. lipolytica* AN-L15 (sample taken at 42 h). Chromatograms were acquired at 36°C, and absorbance was detected at (A) 254 nm and (B) 476 nm (reference wavelength, 360 nm). The numbers above the peaks correspond to compounds shown in Fig. 3 and Table 1. Note the significantly higher absorbance of the TNT-hydride complexes at 476 nm. mAU, 10^{-3} absorbance units.

eight detected hydride complexes, as well as TNT, 2-HADNT, and 4-HADNT. The ADNTs, which eluted after TNT and the hydroxylamino-dinitrotoluenes, are not shown in Fig. 2 (Table 1 shows the retention times) since they were never observed concurrently with all eight detected hydride complexes. The proposed pathways of TNT conversion by strain AN-L15 are shown in Fig. 3.

Metabolites formed during nitro group reduction of TNT. Figures 1B and C show the concentrations of TNT and its conversion products during yeast growth. The total observed concentrations of 2-HADNT (compound 9) (Fig. 3 and Table 1), 4-HADNT (compound 11), 2-ADNT (compound 12), and 4-ADNT (compound 13) did not exceed 47, 56, 6, and 9 μM (after 60 h), respectively, or accounted for less than 27% of the added TNT (440 μM). This indicates that nitro group reduction has a minor role during TNT transformation by *Y. lipolytica* AN-L15. Nitro group reduction appears to occur preferentially at the *para* position instead of the *ortho* position, as described previously for direct biological reduction (2, 3, 6). Retention times, major mass fragments observed during APCI-MS, and UV-visible absorbance maxima for 2-HADNT, 4-HADNT, 2-ADNT, and 4-ADNT are shown in Table 1 and matched those of chemical standards. APCI-MS of the hydroxylamino-dinitrotoluenes showed a major ion at *m/z* 212 (proton loss during negative-mode APCI-MS), as well as another ion at *m/z* 197; APCI-MS of the ADNTs resulted in a major peak at *m/z* 196 (loss of a proton during negative-mode APCI-MS).

Metabolites produced during direct aromatic ring reduction of TNT. TNT aromatic ring reduction by *Y. lipolytica* AN-L15 occurred at both the C-3 and C-1 positions and resulted in the accumulation of two red TNT-monohydride complexes that could be separated using the HPLC method described above. The C-3 hydride complex of TNT (3-H^--TNT, compound 7) was identified based on its UV-visible absorbance spectrum with maxima (λ_{max}) at 256, 480, and 550 nm (Table 1) and on a comparison to previously published results (19). After 24 h, approximately 260 μM 3-H^--TNT was produced by strain AN-L15 cells (Fig. 1B). Since TNT-hydride complexes are not easily stabilized and thus not commercially available for standardization, the estimate of 260 μM 3-H^--TNT was the result of a one-point calibration based on the observation that during the first 6 h of TNT transformation, only 3-H^--TNT and 4-HADNT were observed. Hence, the concentration of 3-H^--TNT after 6 h was estimated based on the disappearance of TNT (60 μM) and the formation of 4-HADNT (4 μM). The remainder was attributed to 3-H^--TNT, a response factor cal-

TABLE 1. Metabolites detected during TNT transformation by *Y. lipolytica* AN-L15

Compound		Negative-mode APCI-MS ions (*m/z*)[a]	HPLC retention time (min) at[b]:		Spectrophotometry λ_{max} (nm)[c]
No.	Description		36°C	50°C	
1	3-H^--TNT isomer	181, 197, 211, **227**	4.8	4.7	261, 445
2	3,5-2H^--TNT·H^+ isomer	183, 196, 211, **230**	5.2	4.9	266, 426
3	3,5-2H^--TNT·H^+ isomer	185, 196, 212, **230**	5.3	5.0	263, 478
4	3,5-2H^--TNT	181, 197, 211, **228**	5.7	5.4	325, 512
5	3-H^--TNT isomer	182, 197, 211, **227**	5.9	5.5	262, 465
6	3,5-2H^--TNT·H^+ isomer	185, 196, 211, **230**	6.7	6.2	263, 491
7	3-H^--TNT isomer	181, 197, 211, **227**	9.9	8.5	256, 480, 550
8	1-H^--TNT	182, 197, 212, **227**	12.3	10.3	251, 478, 551
9	2-HADNT	197, **212**	14.8	12.4	228, 265, 356
10	TNT	197, 211, **227**	15.4	13.3	230
11	4-HADNT	197, **212**	16.0	13.3	232, 350
12	2-ADNT	**196**	17.0	14.1	225, 270, 375
13	4-ADNT	**196**	17.6	14.7	235, 362

[a] Ions detected during negative-mode APCI-MS analyses. Bold type indicates the molecular ion; underlining indicates the main ion observed.
[b] Retention times observed at two different separation temperatures. Details of the HPLC method are described in Materials and Methods.
[c] UV-visible absorbance maxima.

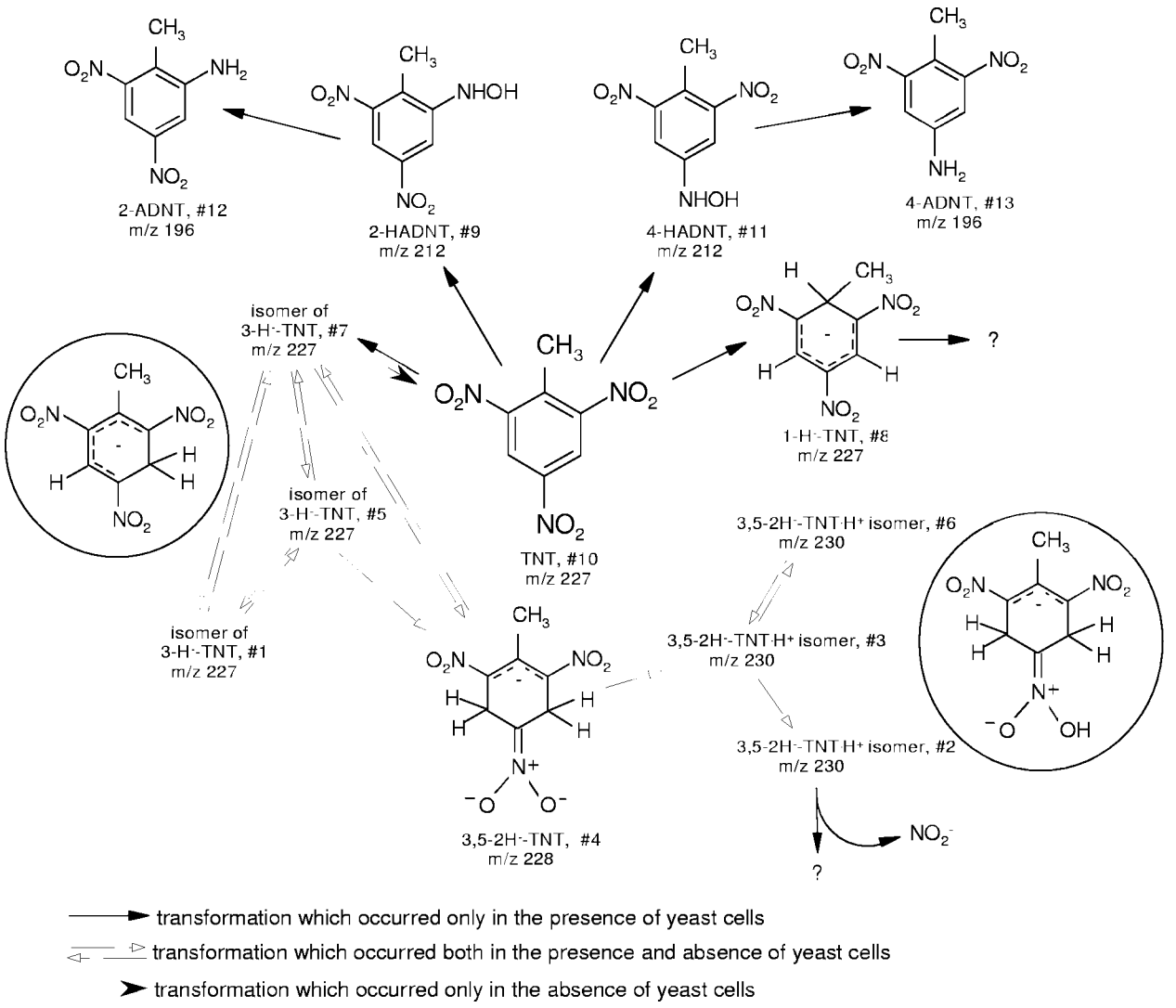

FIG. 3. Proposed pathways of TNT transformation in the presence of *Y. lipolytica* AN-L15. Compounds are numbered according to their elution order during HPLC analysis at 36°C. Data obtained in this study did not allow structural distinction between the different 3-H^--TNT or 3,5-2H^--TNT·H^+ isomers. Structures for these isomers were proposed previously by Vorbeck et al. (20) and Stenuit et al. (18), and one representative structure for each group of isomers is shown in a circle. Compound 8 (1-H^--TNT) was proposed by French et al. (5) but was not characterized in previous work.

culated and used for estimation of 3-H^--TNT concentrations throughout this study.

The second red metabolite (compound 8) (Fig. 3) is suggested to be the C-1 hydride complex of TNT (1-H^--TNT) and was baseline separated from 3-H^--TNT during HPLC analysis (Fig. 2). Compound 8 was observed during approximately the same timeframe as 3-H^--TNT, although with significantly smaller peak areas (Fig. 1C). Compound 8 has a UV-visible spectrum (λ_{max}, 251, 478, and 551 nm [Table 1]) very similar to that of 3-H^--TNT, as well as mass spectral characteristics basically identical to those of 3-H^--TNT. APCI-MS analysis of both TNT-monohydride complexes revealed major ions at *m/z* 181 to 182, 197, 211 to 212, and 227. These observations agree with previously published results that identified 3-H^--TNT using MS and nuclear magnetic resonance spectroscopy (19, 22). Based on the similar UV-visible and mass spectral characteristics, compound 8 is proposed to be 1-H^--TNT.

Further transformation of the TNT-monohydride complexes by *Y. lipolytica* AN-L15 was evident due to a color change from dark red to orange and later to yellow, indicating the formation of TNT-dihydride complexes (5, 14, 20). HPLC analysis during this stage of the experiment clearly resolved an additional six peaks (compounds 1 through 6), which are plotted as the sum of their peak areas in Fig. 1C. Each of these six compounds except compound 4, whose first absorbance maximum appeared to be at 325 nm, showed UV absorbance maxima (λ_{max}) in the range from 261 to 266 nm (Table 1). Compound 4 might have an additional absorbance maximum in the range from 260 to 270 nm as well, which could be partially hidden due to the wide absorbance peak around 325 nm (see Fig. S1 in the

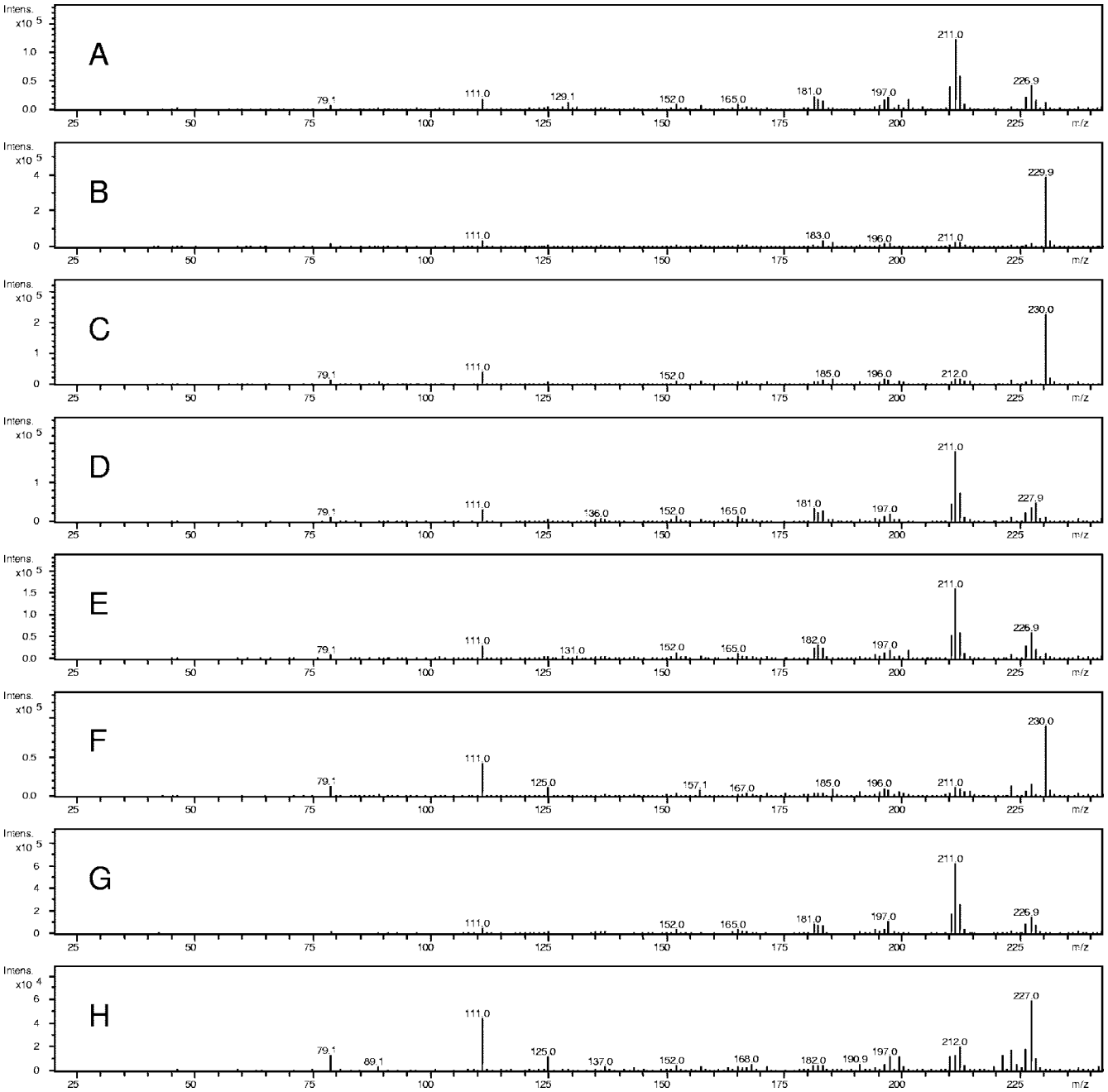

FIG. 4. Mass spectra of TNT-hydride complexes as determined by negative-mode APCI. (A) Compound 1; (B) compound 2; (C) compound 3; (D) compound 4; (E) compound 5; (F) compound 6; (G) compound 7; (H) compound 8.

supplemental material for absorbance spectra). The second and larger absorbance maxima varied more widely among these six compounds, with compound 4 once again having the maximum at the longest wavelength (512 nm); the other five compounds showed λ_{max} between 426 and 491 nm (Table 1). The UV-visible absorbance spectra for the eight hydride complexes detected in this work are summarized in Fig. S1 in the supplemental material.

Figure 4 shows the results of APCI-MS analysis of compounds 1 through 8. The appearance of a base ion at *m/z* 230 for protonated dihydride complexes (compounds 2, 3, and 6) was reported previously by Pak et al. (14) and Vorbeck et al. (20), who used electrospray ionization MS. A molecular ion at *m/z* 227 (compounds 1, 5, 7, and 8) corresponds to the TNT-monohydride complexes that lost a proton during negative chemical ionization. The mass spectrum with a base ion at *m/z* 228 (compound 4) indicates that a proton was lost from the TNT-dihydride complex (3,5-2H$^-$-TNT) during negative chemical ionization.

Abiotic conversion of TNT-hydride complexes. In order to assess the relative importance of biotic (enzymatic) and abiotic conversion of hydride complexes during TNT transformation

TABLE 2. Abiotic conversion of TNT-hydride complexes after 24 h of incubation at pH 7 in the absence of yeast cells

Compound detected[b]	% of initial peak area[a]							
	Compound 1	Compound 2	Compound 3	Compound 4	Compound 5	Compound 6	Compound 7	Compound 8
1	70				67.5		1.5	
2		95	29	3				
3			57	2		84		
4				76	2		1	
5	23				20		1	
6			14			16		
7	7			18	9		11	
8								98
TNT				1	1.5		85.5	

[a] Compounds 1 to 8 were collected with an automated fraction collector after HPLC separation, vacuum dried, redissolved in phosphate buffer (pH 7.0), and incubated in the absence of yeast cells at 30°C for 24 h.
[b] Compound detected after 24 hours.

by *Y. lipolytica* AN-L15, the TNT-monohydride complexes (compounds 7 and 8) were collected after HPLC separation, vacuum dried, and redissolved in phosphate buffer (pH 7.0). No transformation of these compounds was observed during drying and redissolution in phosphate buffer, as confirmed by HPLC analysis. Aerobic incubation of 1-H^--TNT (compound 8) in the absence of yeast cells for 24 h at 30°C did not result in the formation of other products (Table 2). The apparent lack of dihydride complex formation from 1-H^--TNT during abiotic and biotic experiments could have been due to the low concentration observed (the maximum peak area never exceeded 4% of the sum of the areas of the monohydride complexes detected) or the inability of *Y. lipolytica* AN-L15 to further reduce the aromatic ring after 1-H^--TNT formation.

Abiotic transformation of 3-H^--TNT (compound 7) resulted in the appearance of TNT, as well as small amounts of compounds 1, 4, and 5 (Table 2). It has been shown previously that abiotic conversion of 3-H^--TNT leads to TNT (compound 10) production (14, 19). In addition, isomerization of 3-H^--TNT and its disproportionation resulted in the production of compounds 1, 4, and 5. The UV-visible spectral characteristics of 3,5-2H^--TNT (compound 4) were described previously by Vorbeck et al. (20). However, the UV-visible absorbance spectrum of the compound suggested to be 3,5-2H^--TNT in the study of these workers is different from the spectrum reported here (compound 4) (Table 1; see Fig. S1 in the supplemental material). The absorbance maxima reported by Vorbeck et al. for 3,5-2T^--TNT were 267 and 445 nm, and the absorbance maxima observed here were 325 and 512 nm. The differences in the absorbance spectra could have been due to differences in the solvent used for absorbance measurement, as well as the unstable nature of TNT-hydride complexes, which could have led to the formation of (protonated) isomers or tautomers of 3,5-2H^--TNT immediately prior to or during the measurements. Furthermore, as described above, there may be additional absorbance maxima around 267 and 445 nm for compound 4, but they are smaller than the major maxima around 325 and 512 nm. Compounds 1 and 5 are possible isomers of 3-H^--TNT, and their chemical structures were suggested to be resonance forms by Stenuit et al. (18); however, their HPLC retention times, mass, and UV-visible spectra have not been described previously.

Abiotic incubation of 3,5-2H^--TNT (compound 4) resulted in the appearance of 3-H^--TNT (compound 7), small amounts of TNT (compound 10), and the production of compounds 2 and 3 (3,5-2H^--TNT·H^+ isomers). Abiotic conversion of compound 5 resulted in the formation of compounds 1 and 7 (3-H^--TNT isomers), as well as small amounts of 3,5-2H^--TNT (compound 4) and TNT (compound 10); transformation of compound 1 resulted in the appearance of compounds 5 and 7 (3-H^--TNT isomers). Compound 3 was converted abiotically into compounds 2 and 6 (3,5-2H^--TNT·H^+ isomers). Compound 6 appeared to be converted exclusively into compound 3; however, the apparent lack of production of compound 2 from compound 6 was likely due to a low initial starting concentration of compound 6 and slow reaction kinetics for conversion of compound 6 to compound 3. In additional experiments in which the initial concentration of compound 6 was higher, traces of compound 2 were observed after 24 h (data not shown). Abiotic incubation of purified compound 2 did not result in the production of any other hydride complexes, indicating that this compound is a stable TNT transformation product at pH 7.0 in the absence of *Y. lipolytica* (Table 2).

Release of nitrite during TNT aromatic ring reduction in the presence of *Y. lipolytica*. The release of nitrite (NO_2^-) was observed during TNT conversion by *Y. lipolytica* AN-L15 (Fig. 1B). Nitrite was first detected at the onset of TNT-hydride complex production, and the nitrite concentration continued to increase even after disappearance of 1-H^--TNT and complete transformation of 3-H^--TNT to other hydride forms (Fig. 1). Approximately 7% (88 μM) of the theoretical amount of nitrite added as TNT (440 μM TNT, equivalent to 1,320 μM nitrite) was released during the first 84 h of incubation, and the nitrite concentration continued to increase thereafter. Other potential products of TNT denitration, such as dinitrotoluenes or ADMTNBs (9, 11, 14), were not detected. Control experiments without TNT verified that nitrite production by *Y. lipolytica* was due to denitration of TNT and not due to nitrification of ammonium present in the medium (data not shown). Hence, it appears that the source of nitrite is one of the dihydride isomers.

In the presence of yeast cells incubation of all HPLC-purified TNT-hydride complexes except 1-H^--TNT resulted in transient accumulation of compound 2 and its subsequent disappearance. Nitrite continued to be produced at least until all 3-H^--TNT-related hydride complexes had disappeared (data

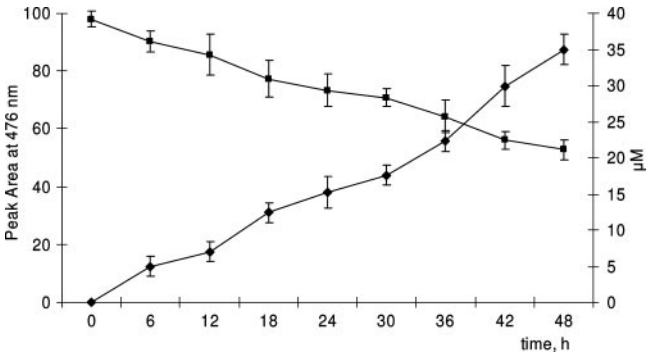

FIG. 5. Nitrite accumulation during degradation of HPLC-purified 3,5-2H$^-$-TNT·H$^+$ (compound 2). Compound 2 was added to synthetic medium and incubated in the presence of yeast cells (initial A_{600}, 0.2). Symbols: ■, compound 2 (detection at 476 nm); ◆, nitrite ion (μM).

not shown). Figure 5 demonstrates the release of nitrite from compound 2; no other TNT-hydride complexes were observed during this experiment. This experiment, along with the abiotic TNT-hydride complex transformation experiments, clearly indicated that the enzyme(s) produced by *Y. lipolytica* AN-L15 is responsible for the release of nitrite from the protonated TNT-dihydride complexes and that compound 2 is the most likely source of nitrite release. However, the exact reason for the development of an enzyme system capable of catalyzing the release of nitrite from the hydride complexes is uncertain. Since strain AN-L15 was unable to grow with TNT as its sole source of carbon or nitrogen (data not shown), TNT conversion appears to be a cometabolic process.

DISCUSSION

TNT contamination of water and soil is a worldwide problem (15). Accurate prediction of the fate of this compound and transport in the environment, as well as improved remediation technologies, depend on a thorough understanding of its biotic and abiotic transformation in natural systems. Recent efforts (1, 2) have demonstrated the utility of drastically improved chromatographic separation for the identification of intermediates formed during conversion of TNT via nitro group reduction. The research presented here capitalized on the improved chromatographic methods and combined them with MS analysis to obtain an improved understanding of TNT transformation mechanisms during aromatic ring reduction.

Prior to nitrite release and the potential cleavage of the aromatic ring, a number of so-called TNT-hydride complexes are produced by the yeast strain *Y. lipolytica* AN-L15. Previously published research investigating the direct aromatic ring reduction of TNT described five hydride complexes, including 3-H$^-$-TNT, 3,5-2H$^-$-TNT, and three protonated isomers of 3,5-2H$^-$-TNT (14, 20, 21). The research described here revealed eight TNT-hydride complexes, which were characterized based on their HPLC retention times, UV-visible absorbance spectra, and mass fragmentation patterns.

Yinon and colleagues analyzed chemically synthesized 3-H$^-$-TNT using electron impact and chemical ionization MS (22). They reported that negative chemical ionization fragmentation ions at *m/z* 182, 197, 210, and 227 are characteristic of 3-H$^-$-TNT and that *m/z* 182 is the distinguishing difference between TNT and 3-H$^-$-TNT. The *m/z* 210 ion was suggested to be a result of OH$^-$ group elimination from 3-H$^-$-TNT, the appearance of the ion at *m/z* 197 was described to be related to the loss of an NO group as a result of a reduction process, and the *m/z* 182 ion was a result of 3-H$^-$-TNT hydrolysis associated with the possible loss of a nitro group. Our negative-mode APCI-MS analysis resulted in very similar fragmentation patterns for TNT and 3-H$^-$-TNT and confirmed that the *m/z* 182 ion can be used to distinguish between these two compounds.

The abiotic conversion of 3-H$^-$-TNT was described previously. Vorbeck et al. (19) and Pak et al. (14) demonstrated the spontaneous abiotic transformation of chemically synthesized 3-H$^-$-TNT. However, TNT was detected as the only product of this transformation, and no other hydride complexes were described. Our research clearly supports the findings of Vorbeck et al. and Pak et al. but also demonstrates that 3-H$^-$-TNT (compound 7) abiotically transforms into its isomers (compounds 1 and 5, suggested by Stenuit et al. [18]), as well as into its dihydride form (compound 4). Furthermore, three additional TNT-hydride complexes were detected. Although our data are not sufficient to determine the exact chemical structure of compounds 1, 2, 3, 5, and 6 (Fig. 3), we demonstrated that these compounds exhibit mass and UV-visible absorbance spectra that strongly resemble those of previously suggested TNT-hydride complexes (5, 14, 20).

French et al. (5) reported that the pentaerythritol-tetranitrate reductase of *E. cloacae* PB can carry out TNT transformation via both hydride attack on the aromatic ring and direct nitro group reduction. 3-H$^-$-TNT was the predominant product of the initial hydride ion-mediated TNT conversion by this reductase, and trace amounts of another metabolite with similar spectral characteristics were detected. This compound was suggested to be 1-H$^-$-TNT, although this suggestion was not confirmed in subsequent work by the same group (21).

In previous work with *Y. lipolytica* NCIM 3589 (9), accumulation of nitrite during TNT transformation occurred via denitration of the 3-H$^-$-TNT complex along with simultaneous production of 2,4-DNT. However, the presence of TNT-hydride complexes was monitored solely by spectrophotometry by Jain et al. (9), and there was no chromatographic separation of these metabolites; hence, the transformation products and mechanisms involved in nitrite release remained unknown.

Pak et al. (14) reported the production of NO_2^- and ADMTNBs in the presence of the XenB reductase of *P. fluorescens* I-C during TNT transformation. They proposed that the accumulation of ADMTNBs was a result of nonenzymatic reactions between intermediates of TNT nitro group and aromatic ring reduction. In TNT transformation experiments with *Escherichia coli*, Stenuit et al. (17) also observed the elimination of nitrite from TNT and the simultaneous production of ADMTNBs and confirmed the presence of these compounds with ^{15}N-labeled TNT. They, however, suggested that *E. coli* is not capable of producing hydride complexes from TNT, thus implying that there is a different pathway for the release of nitrite. Williams et al. (21) reported nitrite release simultaneous with disappearance of "the orange products" and without accumulation of 2,4-DNT or ADMTNBs in TNT transformation experiments with *E. cloacae* and *E. coli* enzymes. They suggested that one of the protonated TNT-dihydride com-

plexes undergoes a transformation to yield nitrite and an alcohol or a ketone (21). However, nitrite release in the work of Williams et al. (21) was assayed spectrophotometrically using the Griess reagent, which was refuted to be a possible reagent for nitrite quantification by Vorbeck et al. (20).

Nitrite release in our work was measured using ion chromatography and was observed not only during the disappearance of the orange products (dihydride complexes) but also during the accumulation of 3-H^--TNT and 1-H^--TNT. Although 88 μM nitrite was detected during TNT transformation by *Y. lipolytica* AN-L15, neither 2,4-DNT nor ADMTNBs were detected. Thus, it is possible that TNT was transformed to alcohols or ketones, as proposed by Williams et al. (21).

This research project utilized HPLC-diode array detection combined with fraction collection and negative-mode APCI-MS for identification of TNT nitro group and direct aromatic ring reduction products formed by *Y. lipolytica* strain AN-L15. Three TNT-hydride complexes which had not been detected in previous work were detected and characterized. The ability to detect these TNT transformation products separately should be important in the future since it should help workers obtain a better understanding of the mechanisms of TNT aromatic ring cleavage and nitrite release and ultimately improve bioremediation of explosives.

ACKNOWLEDGMENTS

This work was supported by a Fulbright graduate student fellowship to Ayrat Ziganshin (Institute of International Education grantee 15061570). Partial financial support was provided by the U.S. Department of Defense Army Research Office (grant DAAD19-03-C-0103). We also acknowledge Defense University Research Instrumentation Program contract W911NF0510255.

John Neuman's indispensable help with the analytical procedures is gratefully acknowledged. Also, the time and effort of the anonymous reviewers, who contributed significantly to improvement of the manuscript, are gratefully acknowledged.

REFERENCES

1. **Borch, T., and R. Gerlach.** 2004. Use of reversed-phase high-performance liquid chromatography–diode array detection for complete separation of 2,4,6-trinitrotoluene metabolites and EPA Method 8330 explosives: influence of temperature and an ion-pair reagent. J. Chromatogr. A **1022:**83–94.
2. **Borch, T., W. P. Inskeep, J. A. Harwood, and R. Gerlach.** 2005. Impact of ferrihydrite and anthraquinone-2,6-disulfonate on the reductive transformation of 2,4,6-trinitrotoluene by a gram-positive fermenting bacterium. Environ. Sci. Technol. **39:**7126–7133.
3. **Esteve-Nunez, A., A. Caballero, and J. L. Ramos.** 2001. Biological degradation of 2,4,6-trinitrotoluene. Microbiol. Mol. Biol. Rev. **65:**335–352.
4. **Fiorella, P. D., and J. C. Spain.** 1997. Transformation of 2,4,6-trinitrotoluene by *Pseudomonas pseudoalcaligenes* JS52. Appl. Environ. Microbiol. **63:**2007–2015.
5. **French, C. E., S. Nicklin, and N. C. Bruce.** 1998. Aerobic degradation of 2,4,6-trinitrotoluene by *Enterobacter cloacae* PB2 and by pentaerythritol tetranitrate reductase. Appl. Environ. Microbiol. **64:**2864–2868.
6. **Hawari, J., A. Halasz, L. Paquet, E. Zhou, B. Spencer, G. Ampleman, and S. Thiboutot.** 1998. Characterization of metabolites in the biotransformation of 2,4,6-trinitrotoluene with anaerobic sludge: role of triaminotoluene. Appl. Environ. Microbiol. **64:**2200–2206.
7. **Hawari, J., A. Halasz, S. Beaudet, L. Paquet, G. Ampleman, and S. Thiboutot.** 1999. Biotransformation of 2,4,6-trinitrotoluene with *Phanerochaete chrysosporium* in agitated cultures at pH 4.5. Appl. Environ. Microbiol. **65:**2977–2986.
8. **Huang, S., P. A. Lindahl, C. Wang, G. N. Bennett, F. B. Rudolph, and J. B. Hughes.** 2000. 2,4,6-Trinitrotoluene reduction by carbon monoxide dehydrogenase from *Clostridium thermoaceticum*. Appl. Environ. Microbiol. **66:**1474–1478.
9. **Jain, M. R., S. S. Zinjarde, D. D. Deobagkar, and D. N. Deobagkar.** 2004. 2,4,6-Trinitrotoluene transformation by a tropical marine yeast, Yarrowia lipolytica NCIM 3589. Mar. Pollut. Bull. **49:**783–788.
10. **Keith, L. H., and W. A. Telliard.** 1979. Priority pollutants: a perspective view. Environ. Sci. Technol. **13:**416–423.
11. **Kim, H.-Y., and H.-G. Song.** 2000. Comparison of 2,4,6-trinitrotoluene degradation by seven strains of white rot fungi. Curr. Microbiol. **41:**317–320.
12. **Michels, J., and G. Gottschalk.** 1994. Inhibition of the lignin peroxidase of *Phanerochaete chrysosporium* by hydroxylamino-dinitrotoluene, an early intermediate in the degradation of 2,4,6-trinitrotoluene. Appl. Environ. Microbiol. **60:**187–194.
13. **Naumov, A. V., E. S. Suvorova, A. M. Boronin, S. K. Zaripova, and R. P. Naumova.** 1999. Transformation of 2,4,6-trinitrotoluene into toxic hydroxylamino derivatives by lactobacilli. Mikrobiologiya **68:**56–62.
14. **Pak, J. W., K. L. Knoke, D. R. Noguera, B. G. Fox, and G. H. Chambliss.** 2000. Transformation of 2,4,6-trinitrotoluene by purified xenobiotic reductase B from *Pseudomonas fluorescens* I-C. Appl. Environ. Microbiol. **66:**4742–4750.
15. **Rieger, P.-G., and H.-J. Knackmuss.** 1995. Basic knowledge and perspectives on biodegradation of 2,4,6-trinitrotoluene and related nitroaromatic compounds in contaminated soil, p. 1–18. *In* J. C. Spain (ed.), Biodegradation of nitroaromatic compounds. Plenum Press, New York, NY.
16. **Spain, J. C., J. B. Hughes, and H.-J. Knackmuss (ed.).** 2000. Biodegradation of nitroaromatic compounds and explosives. Lewis Publishers, Boca Raton, FL.
17. **Stenuit, B., L. Eyers, R. Rozenberg, J.-L. Habib-Jiwan, and S. N. Agathos.** 2006. Aerobic growth of *Escherichia coli* with 2,4,6-trinitrotoluene (TNT) as the sole nitrogen source and evidence of TNT denitration by whole cells and cell-free extracts. Appl. Environ. Microbiol. **72:**7945–7948.
18. **Stenuit, B., L. Eyers, S. E. Fantroussi, and S. N. Agathos.** 2005. Promising strategies for the mineralization of 2,4,6-trinitrotoluene. Rev. Environ. Sci. Biotechnol. **4:**39–60.
19. **Vorbeck, C., H. Lenke, P. Fischer, and H.-J. Knackmuss.** 1994. Identification of a hydride-Meisenheimer complex as a metabolite of 2,4,6-trinitrotoluene by a *Mycobacterium* strain. J. Bacteriol. **176:**932–934.
20. **Vorbeck, C., H. Lenke, P. Fischer, J. C. Spain, and H.-J. Knackmuss.** 1998. Initial reductive reactions in aerobic microbial metabolism of 2,4,6-trinitrotoluene. Appl. Environ. Microbiol. **64:**246–252.
21. **Williams, R. E., D. A. Rathbone, N. S. Scrutton, and N. C. Bruce.** 2004. Biotransformation of explosives by the old yellow enzyme family of flavoproteins. Appl. Environ. Microbiol. **70:**3566–3574.
22. **Yinon, J., J. V. Johnson, U. R. Bernier, R. A. Yost, H. T. Mayfield, W. C. Mahone, and C. Vorbeck.** 1995. Reactions in the mass spectrometry of a hydride Meisenheimer complex of 2,4,6-trinitrotoluene (TNT). J. Mass Spectrom. **30:**715–722.
23. **Zaripov, S. A., A. V. Naumov, E. S. Suvorova, A. V. Garusov, and R. P. Naumova.** 2004. Initial stages of 2,4,6-trinitrotoluene transformation by microorganisms. Mikrobiologiya **73:**398–403.
24. **Zaripov, S. A., A. V. Naumov, J. F. Abdrakhmanova, A. V. Garusov, and R. P. Naumova.** 2002. Models of 2,4,6-trinitrotoluene (TNT) initial conversion by yeasts. FEMS Microbiol. Lett. **217:**213–217.